Power Quality Improvement of Photovoltaic Distributed Generation System using Artificial Neural Network for Environmental Preservation

DOI : 10.36909/jer.ICMET.17185

Anshul Agarwal*, Shubham Kumar Singh, Tirupathiraju Kanumuri and Harish Kumar

National Institute of Technology Delhi, New Delhi, India.

*Email: anshul@nitdelhi.ac.in; Corresponding Author.

ABSTRACT

Most of the economies are emerging with the growth in the renewable energy system. A solar photovoltaic system is one of the good sources of energy among them which provides clean and green energy. As it adds less pollution to the environment and hence advancement in technology of renewable energy system adds great effect on the environmental preservation. This paper describes a 1-ϕ photovoltaic distributed generation system having enhanced power quality features. Initially, the system has been implemented by using pulse width modulation-based switching schemes for the smooth control of the power flow between photovoltaic system, grid, and non-linear load. The system involves nonlinear current compensation and capacitor voltage balancing along with maximum power point tracking. Using this model, sample data has been collected for the training and testing of artificial neural networks. The artificial neural network was trained using the scaled conjugate gradient approach. The response of the neural network provides an estimated reference current for the controller to enhance power quality features. The inverter used in this work also acts as a shunt active power filter during night time. The system's result is simulated and validated through MATLAB/Simulink.

Keywords: Photovoltaic Distributed Generated (PVDG) System; Artificial Neural Network (ANN); Non-linear load; Shunt Active Power Filter (SAPF).

INTRODUCTION

Since conventional centralized generation system uses large generating units to generate electricity most efficiently but this scheme has several drawbacks as the system requires an extensive transmission system and apparatus which uses 6-7% of transmitted power. One of the solutions to this problem is Distributed Generation (DG) system. The DG system which is also known as on-site generation, includes source, power electronic converter, filter, and load (Jain et al. 2018). But as the capacity of these plants increases, the power electronics converters connected to them should operate more efficiently and effectively. It also provides a reliable and clean source of energy to customers with reduced transmission and distribution losses. Distribution generation can be used for a single structure such as a building or it can be a part of a micro-grid (Hu et al. 2019). The advantage of DG System over conventional generation system is different customers add different weights to features of electric power supply. Distributed generation system can help electricity suppliers to fulfill the demand according to the customers (Wang et al. 2011). Because of their small size, distributed generation provides flexibility to adapt, efficient operation, and maintenance (Premkumar et al. 2018). The DG system having conventional sources produce pollution and causes global warming which is a threat to the environment. Hence to preserve the environment from threat, it is necessary to replace conventional sources with renewable sources. RES (renewable energy resources) include hydropower, ocean thermal, biomass, wind, and solar energy. Major renewable energy resources such as wind, hydro etc are available only in few locations whereas solar photovoltaic (PV) is available everywhere. Among renewable energy resources, solar energy is cheap, reliable, and abundant. In the PV system, the sunlight incident on PV panels is converted into electricity directly.

The temperature and irradiance affect the power output of PV panels significantly. For a particular irradiance and temperature, the maximum power available at the PV panel is associated with a unique point on the PV and IV curve. PV module requires power electronics

converters as an interface in between PV panels and load for getting maximum power point on PV curve. DC link voltage is used to feed the AC loads using the inverter. Power electronics converters are also used to regulate the flow of power for stand-alone and grid-tied operations.

MOTIVATION & NOVELTY

Due to the dynamic temperature and irradiance, the operation of the PV system at MPPT becomes complicated. Classical MPPT techniques cannot achieve global maximum power point. Now a day's popularity is increasing for injection of extracted power from PV modules to the grid (Panigrahi et al. 2020). Many PV systems have been tied with the grid to reduce the burden of the grid (Noguchi et al. 1998). The harmonics producing non-linear loads such as UPS, energy-efficient lightings draw nonlinear current from the source i.e. the load current does not follow the source voltage. At the PCC, the non-sinusoidal current distorts voltage (Ma et al. 2019). Due to this distorted voltage, the other loads connected at PCC get affected. Therefore, to mitigate these problems, filters and compensators are required. Active power filters (APF) are now commonly employed to compensate for nonlinear current drawn by harmonic producing (nonlinear) loads (Raouf et al. 2014, Swarnkar et al. 2019). Shunt active power filters are also used to compensate for the harmonic component of current demanded by nonlinear loads (Panda et al. 2015, Rahmani et al. 2010). It also provides reactive power compensation. But, this kind of arrangement is costly and also the hardware of the system remains underutilized. Nowadays DG system with the advancement of power electronics converters and control techniques is capable of enhancing the power quality as well as the power supply needed by the load.

To overcome the above-stated problem following point has been addressed.

- Elimination of filter which makes system bulkier.
- Newly evolved techniques such as artificial neural networks can be more effective and flexible to meet the demand and protect the environment. The model involving such techniques has several advantages over conventional techniques such as data-driven-based control techniques, enhancement in performance with its long operation.
- Using the ANN controller, the system becomes more efficient over time. It provides better performance for harmonic compensation of load and is more accurate to estimate

the reference current.

PROPOSED PVDG SYSTEM

A solar PV panel, DC-DC converter, two 5-level H-bridge cascaded inverters, control unit, nonlinear load, and grid are all part of the proposed PVDG system. The PV Panel is used to extract power from solar irradiance to generate the necessary voltage level, as depicted in figure 1. To get the maximum power out of the PV panel, the system needs to track MPP continuously, which can be done with a DC-DC converter. DC-DC converter performs the function of interface module between PV panel and load (Han et al. 2011, Kumar and Agarwal 2021). The DC-DC converter has been operated using the perturbation and observation technique, allowing the system to run at its maximum power point (MPP) (Tatabhatla et al. 2021, Vinod and Sinha 2014). DC output of the DC-DC converter has been converted to AC using two 5-level cascaded H-Bridge inverters to integrate the PV panel with the load and grid. A neural network has been used to implement the inverter's control mechanism. The inverter of the proposed system performs the function of power quality improvement feature which involves DC link voltage stabilization as well as compensation of harmonics generated by the load. A single phase uncontrolled rectifier with RL load has been used for non-linear load. Both, PV system and grid meet the load demand simultaneously.

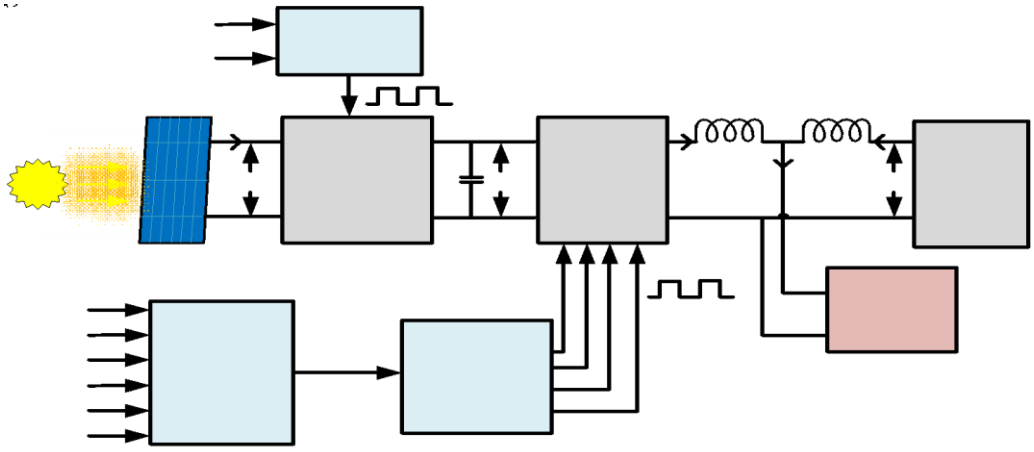

Figure 1. Block schematic of the PVDG system with enhanced PQ features.

The various parameter of the system has been expressed by the following equations.

$$V_{inv} = \sum_{i=1}^{2} V_{DCi}\left(S_{i1} - S_{i2}\right)$$

(1)

Here S_{i1}=S_{i4} and S_{i2}=S_{i3}, where S_{i1}, S_{i2}, S_{i3}, S_{i4} are gate pulse for i^{th} H-bridge inverter.

$$V_{inv} = L_{inv}\frac{dI_{inv}}{dt} + V_P$$

(2)

$$V_G = L_G\frac{dI_G}{dt} + V_P$$

(3)

$$V_P = L\frac{dI_L}{dt} + RI_L - 2V_D$$

(4)

Here L_{inv}, L_G, V_P, V_D are inverter side inductance, grid side inductance, the voltage at the PCC and the voltage drop across diode respectively.

CONTROL SCHEME OF PROPOSED PVDG SYSTEM

Figure 1 depicts a schematic diagram of an enhanced power quality-based PVDG system using an ANN controller. Using perturbation and observation approaches, a DC-DC converter has been employed to accomplish the MPPT of the PV module. In order to convert DC power into AC power, an inverter was employed. As seen in figure 2, the inverter was first controlled using the PWM technique. The study of grid current I_g, load current I_L, and inverter current I_{inv}, as well as active and reactive power, has been done and power quality enhancement features have been combined with the inverter. Using this control technique data have been collected to implement the neural network for better performance.

The load current is obtained from the inverter and grid in load sharing situations and calculated

using the formula given below.

$$I_L = I_{inv} + I_G \tag{5}$$

DC-LINK VOLTAGE REGULATOR AND REFERENCE CURRENT ESTIMATOR

The reference current is estimated for active and reactive power control from DC side to AC side, grid current harmonic compensation and DC-link voltage regulation. The controller as illustrated in figure 2 has been implemented to control the grid current along with DC-link voltage regulation. After filtering the DC-link voltage, it is compared to a set reference voltage (V_{DC}*). The reference current is obtained using the following equations which are used to generate gate pulse using PWM technique.

$$\Delta V(n) = V_{DC}^{*}(n) - V_{DC}(n) \tag{6}$$

$$I_1(n) = I_1(n-1) + K_p[\Delta V(n) - \Delta V(n-1)] + K_I \Delta V(n) \tag{7}$$

Here $I_1(n)$ is the output of PI controller at n^{th} instance, whereas the constants K_P and K_I are proportional and integral constant of PI controller for DC link voltage balancing block.

$$\Delta V_1(n) = \Delta V_{DC1}(n) - \Delta V_{DC2}(n) \tag{8}$$

Here V_{DC1} and V_{DC2} are the output voltage of two PV systems. So the output I_1 of the controller as depicted in figure 2 is given as

$$I_1(n) = I_1(n-1) + K_{p1}[\Delta V_1(n) - \Delta V_1(n-1)] + K_{12} \Delta V_1(n) \tag{9}$$

As a result, the output of DC-link voltage control loop I_V is as follows:

$$I_V(n) = I_1 * V_{gu}(n)$$

(10)

Where $V_{gu}(n)$ is the unit template of grid voltage at n^{th} instant. After that, the load current is added to the equation to provide reference current based on the load requirement.

$$i_{inv}^{ref} = I_V(n) + I_L(n)$$

(11)

This causes the inverter current to track the load current at the previous instant.

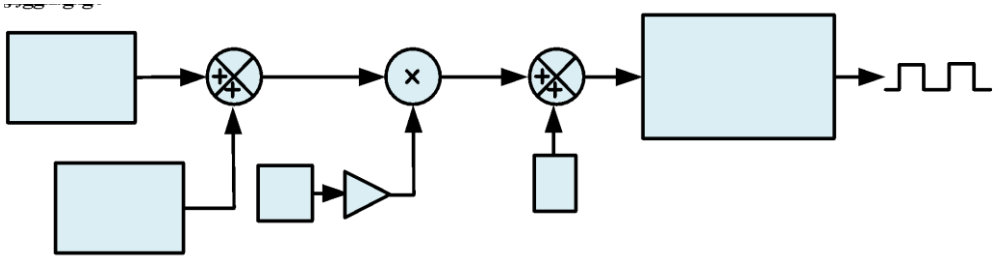

Figure 2. Block diagram of reference current estimator.

ARTIFICIAL INTELLIGENCE

An artificial neural network mimics the behavior of the human brain. So, ANN is used to address the inaccuracy issue of the controller and to achieve estimated reference current effectively artificial neural network controller has been implemented based on training data samples (collected using PWM techniques). Feedforward neural network is one of the popular systems which is used widely (Berrezzek et al. 2020, Saffaran et al. 2020, Yedjour 2020). The neural network was trained using the scaled conjugate gradient approach. The system's parameters such as V_{DC}, I_L, I_G, I_{inv}, V_G, I_{inv}^{ref} as depicted in figure 3, has been used as input for training testing and validation of the neural network model. In this paper, the SCG algorithm has been used to optimize the parameter of the neural network. The neural network's response depends on input training data samples, bias, and weights of the neural network.

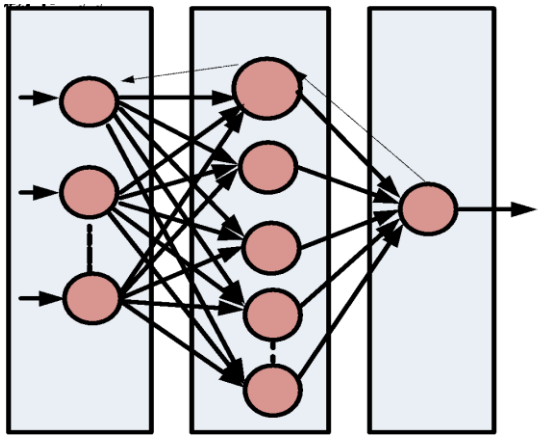

Figure 3. The Neural network model having Scaled Conjugate Gradient algorithm for reference current estimation.

Data samples matrix for the input and response are taken as 10000 by 6 and 10000 by 1 respectively. Data samples are processed through the input layer and the O_i is the output of the input layer. As shown in figure 3 weighted sum of the O_i (inputs of hidden layer neuron) is computed with corresponding weights w_{ij} and bias b at hidden node h_j, denoted by Ih_j (see equation (12)). The output of hidden node Oh_j is calculated using equation (13). At each input node Y_k, the weighted sum of output Oh_j of the hidden node with corresponding weights U_{jk} is computed and represented by IY_k (see equation (15)). Output value OY_k at k^{th} node is computed by equation (16).

$$Ih_j = \left(\sum_{i=1}^{i} w_{ij}.O_i + b \right) \tag{12}$$

$$Oh_j = \left(\sum_{i=1}^{i} w_{ij}.O_i + b \right) \log sigmoid \tag{13}$$

$$Iy_k = \left(\sum_{j=1}^{j} U_{jk}.Oh_j + U \right) \tag{14}$$

$$Oy_k = \left(\sum_{i=1}^{i} U_{ik}.Oh_i + U \right) \log sigmoid \tag{15}$$

The corresponding estimated reference current is obtained in the output layer using equation (16).

$$I_{inv}^{ref} = Oy_k \tag{16}$$

RESULTS

In this paper, the simulation of the model includes harmonic current compensation, power factor correction at the grid, and active and reactive power flow through the proposed PVDG system. Initially, the PWM control technique for the PVDG system is implemented with MATLAB/Simulink, and the reference compensating current is derived using the measured grid voltage, load current, and the DC-link voltage of the two-level PV inverter. The non-linear load consisting of an uncontrolled rectifier with RL elements having R=10 Ω, L=10mH on the DC side, has been considered as the local load for the PV inverter. Figure 4 depicts the system's output, which includes DC link voltage, load current, grid current, and inverter current. The performance has been explored for THD improvement and compensation of reactive power for non-linear loads as depicted in figure 5 to figure 7. The load current requirement is divided into two components namely linear and nonlinear components. The linear component is supplied from the grid and the nonlinear component of load requirement is given from the PV inverter. The operation of the model contains two modes.

Mode 1

In this mode, MPPT is turned on and the PQEC feature is turned off. In figure 5 first mode is simulated from t = 0.1 to t = 0.3 sec. So, the PV inverter does not supply any harmonic component required by the load. It converts available DC power to AC to feed the load. The harmonic content of load is supplied from the grid. In this mode, the extra load requirement is fulfilled by the grid.

Mode 2

In this mode, both MPPT and power quality enhanced feature is turned on. In figure 5, mode 2 is started from t=0.3 sec onwards. The inverter supplies both a linear and a non-linear load current component (required by the load). The grid provides the remaining linear component required by the load. As depicted in figure 5, from 0.5 onwards system shows steady state output. Figure 6

and figure 7 depict the harmonics of grid current and voltage at PCC for non-linear load having R=10 Ω, L=10mH.

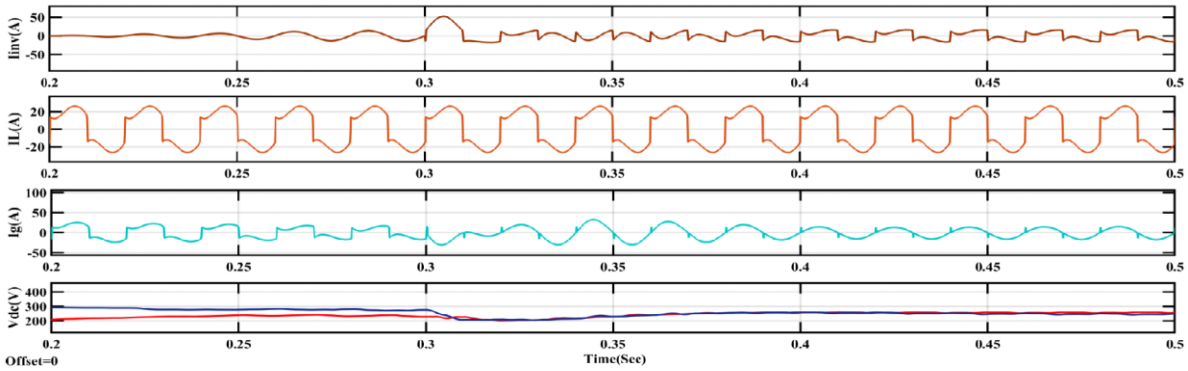

Figure 4. Output Waveforms having two 5-level cascaded MLI as shunt active power filters for the grid-connected photovoltaic system with the non-linear load.

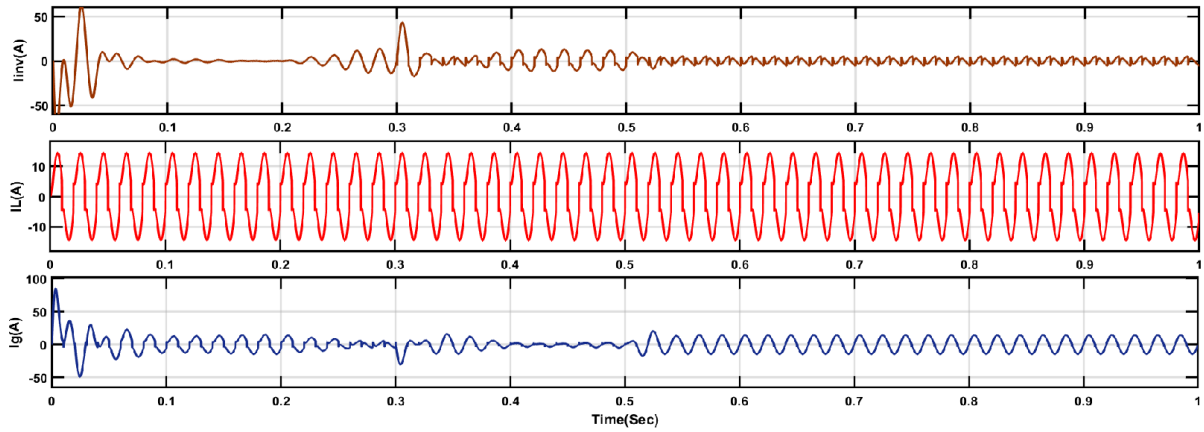

Figure 5. Output waveforms of the inverter, load, and grid current for a different mode of operation for non-linear load having R=10 Ω, L=10mH.

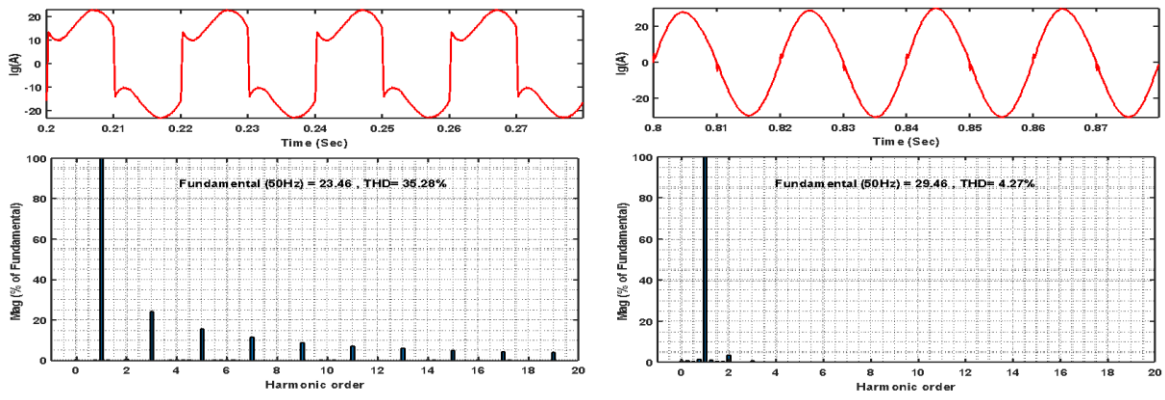

(a) (b)

Figure 6. Spectrum of grid current during operation of (a) mode 1 and (b) mode 2 for non-linear load having R=10 Ω, L=10mH.

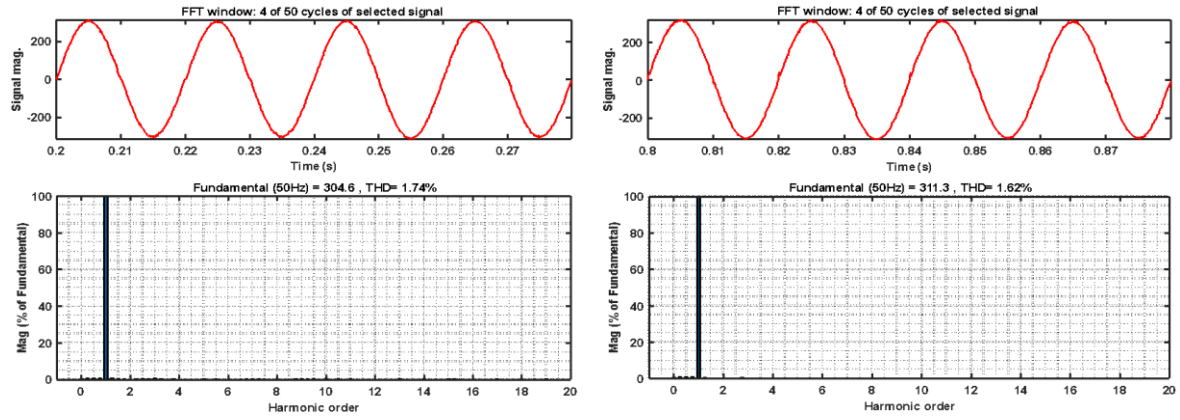

(a) (b)

Figure 7. Harmonic spectrum for PCC Voltage during operation of (a) mode 1 and (b) mode 2 for non-linear load having R=10 Ω, L=10mH.

In steady-state IG has THD = 4.27% and VP has THD = 1.62% for non-linear load having R=10 Ω, L=10mH. THD of grid current and voltage at PCC is given in figure 6 and figure 7 respectively. No power is available at the PV panel during the night and hence in this case the PV inverter works as SAPF. The non-linear current and reactive power demands of the load are compensated by the PV inverter. The grid has to provide only the active and linear components of the load requirement. I_L has a THD requirement of 35.28% of its fundamental component out of which I_g supplies 29.46A with 4.27% THD and I_{inv} supplies the remaining nonlinear component of load current.

The feed forward neural network is structured using six inputs and one output. In the hidden layer of the neural network, there are a distinct number of neurons. The number of neurons in the hidden layer have been chosen depending on the neural network's training and testing. The number of training epochs and MSE were also used to determine the optimal number of hidden layer neurons. Several tests have been carried out in order to find the best hidden layer neuron. A sigmoid function has been used for the hidden layer neuron. The result shown in figure 4 and estimated current is used to collect data for the implementation of an artificial neural network. Ten thousand data samples have been used to train the neural network using the Scaled conjugate gradient technique.

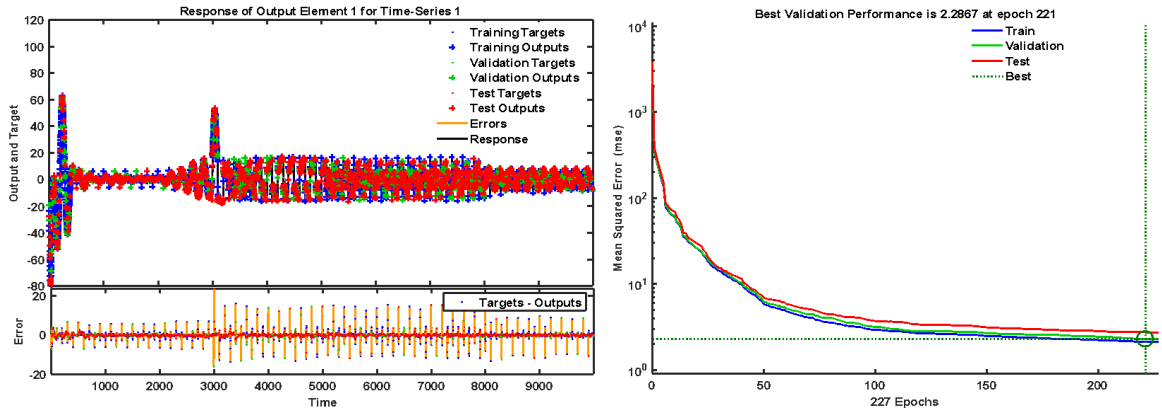

(a) (b)

Figure 8. Output: (a) neural network response for reference current estimator, (b) The neural network's performance in terms of MSE.

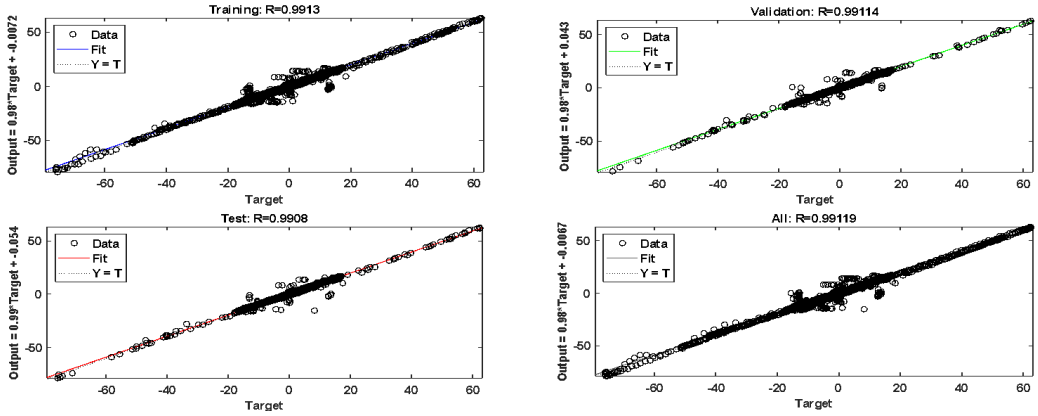

Figure 9. Represents fitting of output and target.

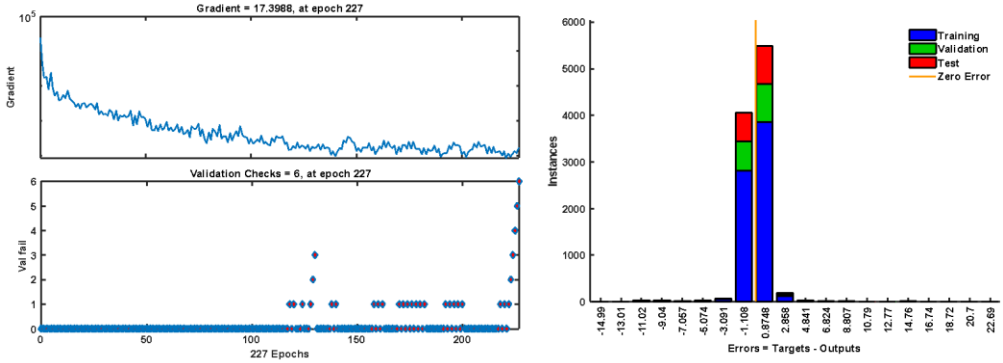

(a) (b)

Figure 10. Output: (a) Variation of gradient error and validation checks of the neural network at epoch 227, (b) represents error histogram at epoch 227.

The output of the neural network is a reference compensating current estimator as depicted in figure 8(a). The neural network has been trained repeatedly to track the estimated reference current until satisfactory performance is achieved. Once the neural network parameter is optimized, the

controller has been validated and tested to track the estimated reference current with less error. Figures 8(a) and 8(b) show the neural network output, training, testing validation. As shown in figure 8(b), the output layer is capable to minimize MSE and the best validation performance is 2.2867 at 221 epoch. Figure 9 shows the Regression analysis of the artificial neural network which represents the fitting of output and target. It also shows the Regression value R is 0.9913 which means the actual output and target of the neural network are much closer. Similarly, Regression analysis has been done for validation and testing the neural network for 227 epochs as depicted in figure 9 respectively. The regression value for validation and tasting are 0.99114 and 09908 respectively. Figure 10 (a) and 10 (b) shows training to state and error histogram at 227 epoch for the artificial neural network. Figure 10 (a) shows the variation of gradient error and validation checks at each instant of 227 epoch. As shown in figure 10 (a) variation of gradient error is 17.3988 whereas 6 validation checks are found at epoch 227. Figure 10 (b) shows the error histogram for output and target. The error lies in between -2 to 1 for most of the data. Neural network training was stopped at 227 epoch. The I_{inv}^{ref} is used to generate the gate pulse of the inverter which supplies the load. The parameter of the artificial neural network is being updated at each iteration and hence system improves itself over time. As depicted in figure 6 and 7, the proposed system eliminates the requirement of filter for nonlinear load effectively.

CONCLUSION

The work proposed a one-photovoltaic (PVDG) system with improved power quality features using an artificial neural network which requires the generation of estimated current accurately. The system has been designed to eliminate the harmonics generated by load without filter. The simulation base studies able to decrease THD for the non-linear load. For the load having R=10 Ω and L=10mH, THD of grid current decreases from 35.28% to 4.27%. DC-link capacitor voltage balancing is also being achieved. The neural network's performance has been tested and validated in MATLAB/Simulink. It is observed that the proposed system eliminated the need for filter for the load and the cost of the system is also being reduced. Hence the proposed system is

economical as well as one of the solution to reduce greenhouse gas to preserve the environment.

REFERENCES

Berrezzek, F., Khelil, K., & Bouadjila, T. 2020. Efficient MPPT scheme for a photovoltaic generator using neural network. CCSSP 2020 - 1st Int Conf Commun Control Syst Signal Process 503–507. https://doi.org/10.1109/CCSSP49278.2020.9151551

Han, Y., Xu, L., & Khan, M.M., 2011. Robust deadbeat control scheme for a hybrid APF with resetting filter and ADALINE-based harmonic estimation algorithm. IEEE Trans Ind Electron 58:3893–3904. https://doi.org/10.1109/TIE.2010.2093475

Hu, J., Li, Z., Zhu, J., & Guerrero, J.M., 2019. Voltage Stabilization: A Critical Step Toward High Photovoltaic Penetration. IEEE Ind Electron Mag (2019) 2:17-30.

Jain, S., Jain, N.K., Vaughn, & W.J., 2018. Challenges in meeting all of India's electricity from solar: An energetic approach. Renew Sustain Energy Rev 82:1006–1013.

Kumar, N., & Agarwal, A., 2021. Solar-Grid Connected Single Phase Water Pumping System for Household Application. 59:206–210

Ma, C., Dasenbrock, J., Tobermann, J.C., & Braun, M., 2019. A novel indicator for evaluation of the impact of distributed generations on the energy losses of low voltage distribution grids. Appl Energy 242:674-683. https://doi.org/10.1016/j.apenergy.2019.03.090

Noguchi, T., Tomiki, H., Kondo, S., & Takahashi, I., 1998. Direct power control of PWM converter without power-source voltage sensors. IEEE Trans Ind Appl 34:473–479.

Panda, A.K., & Patel, R., 2015. Adaptive hysteresis and fuzzy logic controlled-based shunt active power filter resistant to shoot-through phenomenon. IET Power Electron 8:1963–1977.

Panigrahi, R., Mishra, S.K., & Srivastava, S.C., 2020. Grid Integration of Small-Scale Photovoltaic Systems in Secondary Distribution Network - A Review. IEEE Trans Ind Appl 3:3178-3195. https://doi.org/10.1109/TIA.2020.2979789

Premkumar, M., Karthick, K., & Sowmya, R., 2018. A comparative study and analysis on conventional solar PV based DC-DC converters and MPPT techniques. Indones J Electr Eng

Comput Sci 11:831-838. https://doi.org/10.11591/ijeecs.v11.i3.pp831-838

Rahmani, S., Mendalek, N., & Al-Haddad, K., 2010. Experimental design of a nonlinear control technique for three-phase shunt active power filter. IEEE Trans Ind Electron 57:3364–3375.

Raouf, M.H., Nowbakht, A., Haddadi, M.B., & Tabatabaei, M.R., 2014. A Review of Control Schemes for Active Power Filters in Order to Power Quality Improvement. Int J Electr Comput Energ Electron Commun Eng 5: 826-829.

Saffaran, A., Azadi, Moghaddam, M., & Kolahan, F., 2020. Optimization of backpropagation neural network-based models in EDM process using particle swarm optimization and simulated annealing algorithms. J Brazilian Soc Mech Sci Eng 42 1:1-14.

Swarnkar, P., Jain, S.K., & Nema, R.K., 2019. Advanced controlling schemes for active power filter. A review Int. J. Emerg. Tech 2019.

Tatabhatla, V.M.R., Agarwal, A., & Kanumuri, T., 2021. Performance Improvement by Mitigating the Effects of Moving Cloud Conditions. IEEE Trans Power Electron 36:4214–4223 (2021). https://doi.org/10.1109/TPEL.2020.3020807

Vinod, A., & Sinha, A.K., 2014. A study on intelligent algorithms for maximum power point tracking in field of wind energy conversion system (review). In 2014 International Conference on Electronics and Communication Systems, ICECS 2014 13:1-4.

Wang, F., Duarte, J.L., Hendrix, M.A.M., 2011. Grid-interfacing converter systems with enhanced voltage quality for micro-grid application concept and implementation. IEEE Trans Power Electron 26:3501–3513. https://doi.org/10.1109/TPEL.2011.2147334

Yedjour, D., 2020. Extracting Classification Rules from Artificial Neural Network Trained with Discretized Inputs. Neural Process Lett 52:2469–2491.